

# Spectrally resolved coherent transient signal for ultracold rubidium molecules

F. Eimer<sup>1,a</sup>, F. Weise<sup>1</sup>, A. Merli<sup>1</sup>, S. Birkner<sup>1</sup>, F. Sauer<sup>1</sup>, L. Wöste<sup>1</sup>, A. Lindinger<sup>1</sup>, R. Ağanoglu<sup>2</sup>, C.P. Koch<sup>2</sup>, W. Salzmann<sup>3,b</sup>, T. Mullins<sup>3</sup>, S. Götz<sup>3</sup>, R. Wester<sup>3</sup>, and M. Weidemüller<sup>3,c</sup>

<sup>1</sup> Institut für Experimentalphysik, Freie Universität Berlin, Arnimallee 14, 14195 Berlin, Germany

<sup>2</sup> Institut für Theoretische Physik, Freie Universität Berlin, Arnimallee 14, 14195 Berlin, Germany

<sup>3</sup> Physikalisches Institut, Universität Freiburg, Hermann Herder Str. 3, 79104 Freiburg, Germany

Received 13 February 2009 / Received in final form 18 June 2009

Published online 24 July 2009 – © EDP Sciences, Società Italiana di Fisica, Springer-Verlag 2009

**Abstract.** We present spectrally resolved pump-probe experiments on the photoassociation of ultracold rubidium atoms with shaped ultrashort laser pulses. The pump pulse causes a free-bound transition leading to a coherent transient signal of rubidium molecules in the first excited state. In order to achieve a high frequency resolution the bandwidth of the pump pulse is reduced to a few wavenumbers. The frequency dependence of the transient signal close to the D1 atomic resonance is investigated for characteristic pump-probe delay times. The observed spectra, which show a pronounced dip for pump-probe coincidence, are interpreted using quantum dynamical calculations.

**PACS.** 33.80.-b Photon interactions with molecules – 32.80.Qk Coherent control of atomic interactions with photons – 42.50.Md Optical transient phenomena: quantum beats, photon echo, free-induction decay, dephasings

## 1 Introduction

The increasing interest in ultracold molecules has led to a variety of approaches to efficient molecule production schemes. Due to the difficulty of extending laser cooling techniques established for atoms to molecules, new pathways had to be explored. While buffer gas cooling [1] and Stark decelerators [2] are techniques to translationally cool existing molecules, alternative techniques assemble cold atoms to molecules using magnetically induced Feshbach resonances [3] or photoassociation by cw-lasers [4–6]. Due to the abundance and diversity of optical transitions in molecules, photoassociation as a purely optical technique promises versatility.

In the photoassociation step an ultracold colliding atom pair absorbs a photon red detuned with respect to the atomic resonance. This free-bound transition at large internuclear distance leads to excited state molecules in highly excited vibrational levels that can subsequently undergo a transition to the electronic ground state. As several theoretical studies point out, the use of laser pulses instead of cw-laser-light bears some advantages [7–9]. Due to their bandwidth it is possible to excite atom pairs over

a larger range of internuclear distances into bound states. Furthermore, the application of sequences of shaped ultrashort pulses allow to transfer the system into deeply bound states which was done experimentally [7]. The pulses proposed by theory for photoassociation have a pulse duration in the picosecond range and are chirped for high transition yield. First experiments using transform-limited and chirped femtosecond pulses could only demonstrate the destruction of molecules [8,9] while experiments using chirped picosecond pulses in the photoassociation step have shown a flux enhancement on a nanosecond timescale [10]. Another study investigated the ultracold photoassociation ionization [11].

In a recent experiment we successfully used shaped femtosecond pulses to photoassociate ultracold rubidium atoms [12]. The observation of photoassociation was confirmed by the work of Petrovic et al. who experimentally and theoretically investigated the excited state dynamics on a larger timescale [13]. It became evident that this process crucially depends on the laser pulse conditions, i.e. the spectral intensity and temporal shape of the pulse.

In order to investigate the spectral contributions, we present here a study on the coherent formation of molecules from colliding ultracold rubidium atoms in a pump-probe configuration (Fig. 1). The spectrum of the transform-limited femtosecond pulses was strongly restricted to a bandwidth of a few wavenumbers to achieve a higher spectral resolution. This leads to a pulse duration in the short picosecond regime (inset of Fig. 1).

<sup>a</sup> e-mail: frauke.eimer@gmx.de

<sup>b</sup> Present address: Fraunhoferinstitut für Physikalische Messtechnik IPM, Heidenhofstraße 8, 79110 Freiburg, Germany.

<sup>c</sup> Present address: Physikalisches Institut, Universität Heidelberg, Philosophenweg 12, 69120 Heidelberg, Germany.

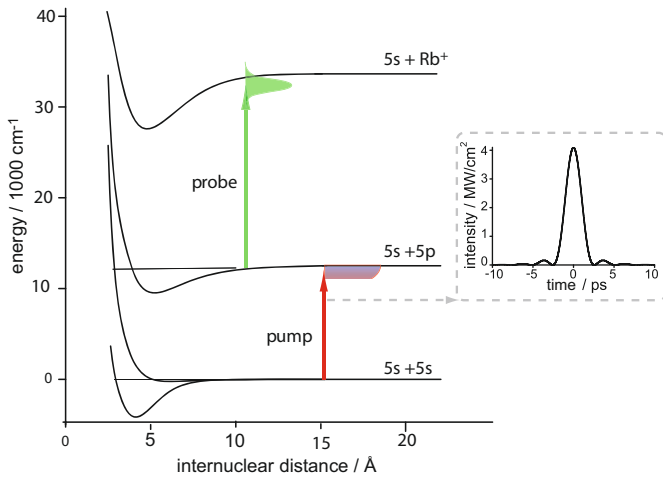


**Fig. 1.** (Color online) Pump-probe excitation scheme for rubidium. The spectral shape of the pulses is indicated qualitatively and the resulting temporal pump pulse for a bandwidth of  $13 \text{ cm}^{-1}$  is depicted in the inset.

## 2 Materials and methods

Our setup consists of a femtosecond laser system and a dark spontaneous force optical trap (dark SPOT) [14]. The background vapour loaded trap captures  $10^8$   $^{85}\text{Rb}$  atoms at densities of  $10^{11} \text{ cm}^{-3}$  and temperatures of  $100 \mu\text{K}$ . The trapping beams excite the  $5 S_{1/2} F'' = 3$  to  $5 P_{3/2} F' = 4$  hyperfine transition while the repump beams excite transitions from  $F'' = 2$  to  $F' = 3$ . In the trap configuration used in the experiments 90% of the trapped atoms are in the dark  $F'' = 2$  ground hyperfine state.

The femtosecond laser system consists of a Coherent MIRA oscillator and a Coherent RegA 9050 amplifier and delivers transform-limited pulses with an energy of  $4 \mu\text{J}$ , and  $25 \text{ nm}$  bandwidth at a repetition rate of  $100 \text{ kHz}$ . To enable two colour pump-probe experiments, the femtosecond pulses are split into two parts.

For the probe pulse 90% of the RegA output power is frequency converted in a non-collinear optical parametric amplifier (NOPA). The center wavelength of the generated probe pulses is tuned to  $488 \text{ nm}$  to allow ionization of molecules in the first excited state. These pulses with a pulse energy of  $10 \text{ nJ}$  have a duration on the order of  $600 \text{ fs}$ .

The remaining smaller fraction of the RegA output power is used for the pump pulse. In order to yield high spectral intensity, the center wavelength is tuned to  $800 \text{ nm}$ . For amplitude modulation the pump pulse passes a zero compression pulse shaper consisting of two gratings of  $2000$  grooves per  $\text{mm}$  and two cylindrical lenses with a focal length of  $250 \text{ mm}$  in a 4-f alignment leading to a resolution of  $0.05 \text{ mm/cm}^{-1}$  in the Fourier plane. Two razor blades inserted in the Fourier plane form a narrow transmission band of  $13 \text{ cm}^{-1}$  width that fully suppresses undesired spectral pulse components. Two precision stages allow the adjustment of the bandwidth and the displacement of the band in the Fourier plane. After passing an optical delay line that allows the adjustment of the temporal

spacing between the pulses they are collinearly overlapped and focussed on the atomic cloud.

Atomic and molecular ions produced by the pulse sequence are extracted from the trap by a constant electric field of  $40 \text{ V/cm}$ , mass selected by an rf quadrupole mass filter, and afterwards detected by a channeltron.

We investigated the dependence of the  $\text{Rb}_2^+$  rate on the pump pulse frequencies close to the D1 atomic resonance for fixed delays between the pump and the probe pulse. For this purpose the transmission band is moved through the pump pulse spectrum in steps of about  $0.5 \text{ cm}^{-1}$ . For each band position the ion rate is averaged over  $10^7$  pump-probe sequences and plotted against the band position relative to the D1 line. The position of the atomic resonance in the Fourier plane is determined with an accuracy of  $1 \text{ cm}^{-1}$  via the fluorescence of the atomic cloud detected with a photodiode. To avoid atom loss due to photon pressure and atomic ionization the laser beam is chopped during the fluorescence measurement. The relative fluorescence (with vs. without beam) reaches its maximum when the spectral filter transmits the atomic resonance.

In order to understand the dependence on the band position, the interaction of the modulated pump pulse with an ultracold pair of colliding atoms was studied theoretically. The time-dependent Schrödinger equation was solved for two diatomic interaction potentials<sup>1</sup> which are dipole coupled by a time-dependent light field. The Hamiltonian was represented on a mapped Fourier grid and the Chebyshev propagator was employed [15]. Interaction with the potential energy curves of the other fine structure component ( $5S+5P_{3/2}$ ) can be neglected since they are energetically well separated at long range.

The electric field of the pump pulse was derived from the Fourier transform of a cut pulse spectrum matching the one used in the experiments. The amplitude modulation with the narrow band changes the temporal shape of the pump pulse drastically. The peak intensity decreases by three orders of magnitude, the pulse duration (FWHM) increases by about a factor of 50 and the mean maximum is accompanied by long oscillating tails (inset of Fig. 1). Since in the experiments the excited state population is monitored via the probe pulse, the calculated time dependent excited population is convoluted with a normalized Gaussian probe pulse with a pulse duration of  $600 \text{ fs}$ .

## 3 Results and discussion

Figure 2 shows the dependence of the molecular ion rate on the pump pulse frequencies at the D1 line for positive, negative, and zero delay of the probe pulse relative to the pump pulse. In the case of positive and negative delay, the molecular ion rate exhibits a peak of plateau-like shape centered at  $1 \text{ cm}^{-1}$ . The ion signal decreases on both sides to a constant and similar background signal. The maximum peak height is achieved at positive delay with the probe following the pump pulse while the peak height obtained with the reverse pulse order is drastically

<sup>1</sup>  $a^3 \Sigma_u^+$  ( $5S+5S$ ) and  $1_g$  ( $5S+5P_{1/2}$ ).

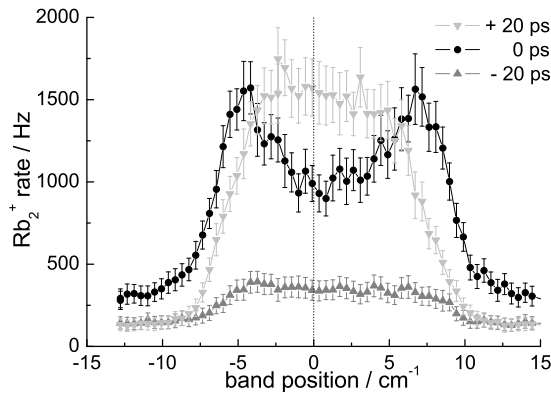


**Fig. 2.** Molecular ion rate depending on the transmission band position relative to the D1 atomic resonance. This is measured for a delay of  $\pm 20$  ps and 0 ps and a bandwidth of  $13 \text{ cm}^{-1}$ . The delay of a probe following a pump pulse is defined as positive.

lower. In both cases the ion signal increases within an interval, whose width roughly mirrors the bandwidth of the modulated pulse.

The occurrence of an increased ion signal at negative delay has been discussed previously and was assigned to ground state molecules which were formed by preceding pulses and spontaneous emission [12]. The ion signal originates from the near resonant ionization of these ground state molecules by a green-red pair of pulses via intermediate states below the  $5S + 4D$  asymptote. Since this signal is due to the repetitive character of the experiments it is not included in the simulations.

In the case of a simultaneous interaction of both pulses two striking differences compared to the delayed cases are visible. Firstly, the ion signal shows an increased peak width compared to the delayed cases. Secondly, instead of one peak the ion signal displays a double maximum with a dip in between just around the atomic resonance. The maximum ion rate reached in the case of pulse coincidence is observed at  $-4 \text{ cm}^{-1}$  and  $7 \text{ cm}^{-1}$  and in the case of positive delay at  $1 \text{ cm}^{-1}$  and amounts to 1600 Hz.

In order to gain more insight into the underlying processes leading to these differences we performed quantum dynamical calculations for the case of positive delay and pulse coincidence. The simulation results depicted in Figure 3 show qualitatively a good agreement with the measurement.

In the case of positive delay the excited state population displays a broad maximum around the atomic resonance that decreases on both sides to zero. The interval in which the excited state population significantly increases matches the bandwidth of the pump pulse.

For the case of pulse coincidence the calculations reproduce the double maximum and the increased peak width. The maximum excited state population in the case of coincidence, reached at  $-5.5 \text{ cm}^{-1}$  and  $+5.5 \text{ cm}^{-1}$ , is about a factor two smaller than the maximum reached in the case of positive delay. The lower experimental values for resonant excitation at positive delay can be explained by a decreased particle density in the ultracold atomic cloud due to photon pressure or atomic ionization. This issue

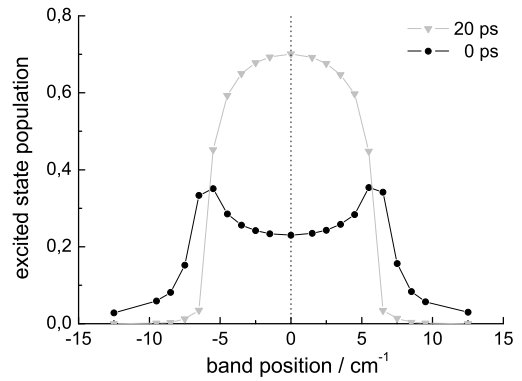


**Fig. 3.** Simulated dependence of excited bound state population on the transmission band position relative to the D1 atomic resonance for a delay of 0 ps (black) and 20 ps (gray) for a bandwidth of  $13 \text{ cm}^{-1}$ .

is also responsible for the more pronounced experimental dip at zero delay compared to the simulations. Comparing the simulations and the experimentally resolved peak-shapes, there is a noticeable shift of about  $1 \text{ cm}^{-1}$  which is, regarding the accuracy of the resonance frequency determination, not significant.

Since the simulations reproduce the peak shapes with good agreement, the time dependence of the calculated population in the excited state for different transmission band positions was investigated (Fig. 4). In all cases the excited state population starts to rise around zero delay and reaches a constant value at 20 ps which determines the peak shape for positive delay in the frequency dependent calculation, cf. Figure 3. The peak shape in the case of coincidence is determined by the population at zero delay. As the calculations show, the delay at which the population rise is maximal crucially depends on the band position. For off-resonant band positions (dotted) i.e. positions where the atomic resonance is blocked, the excited state population rises earlier than in the case of resonant band positions. It reaches its maximum at 0 ps delay and nearly vanishes after the interaction. For the case of off-resonant excitation, population is only transiently transferred to the excited state during the interaction with the pump pulse. This transient contribution to the excited state population leads to the increased peak width in the case of coincidence.

For a symmetric resonant band position ( $0 \text{ cm}^{-1}$ ) the rise is maximally delayed and the population reached at 20 ps exceeds that reached by differing positions. This dependence of the rise on the symmetry of the position relative to the atomic resonance is the origin of the double maximum peak shape for coinciding pulses. The symmetry dependence of the signal rise indicates that for on-resonant band positions destructive interferences are induced between the blue and the red detuned contributions of the pump-pulse. The maximally delayed rise for the symmetric band position can be explained as total destructive interference of the off-resonant contributions. Similar interference effects have been discussed in detail by Dudovich et al. for atoms in a gas cell [16].

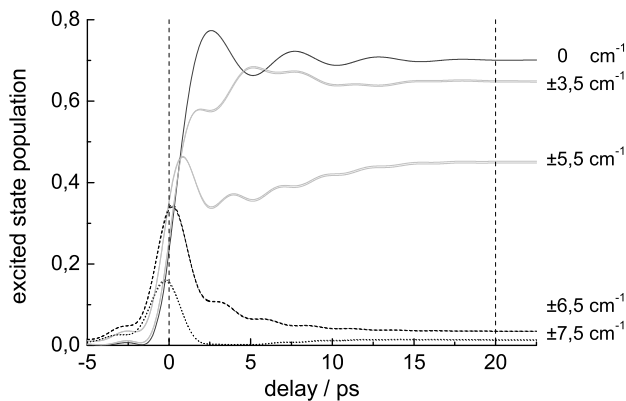


**Fig. 4.** Simulated pump-probe traces for different transmission band positions relative to the D1 atomic resonance. Dotted and solid lines correspond to off-resonant and on-resonant band positions, respectively. The positions with one edge of the band on the atomic resonance are depicted dashed. The vertical lines at 0 ps and 20 ps mark the delay for the static investigation.

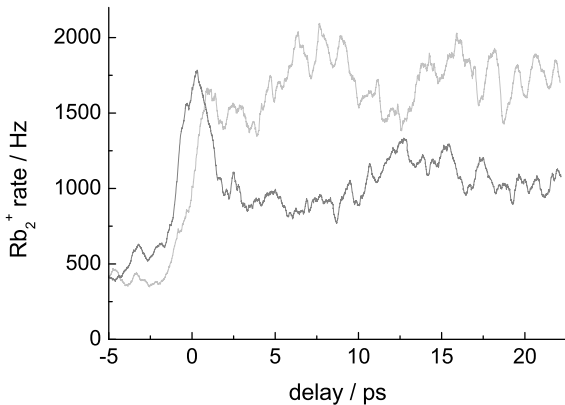


**Fig. 5.** Measured pump-probe traces for a non-symmetric (black) transmission band position at  $7 \text{ cm}^{-1}$  and a more symmetric position at  $-2 \text{ cm}^{-1}$  (gray).

Furthermore, we analysed the characteristic oscillations in the population at positive delay. A Fourier transformation shows that the population is modulated by two frequencies which match the detuning of the transmission band edges relative to the atomic resonance. These coherent molecular transients are related to the induced dipole dynamics observed for atoms by Zamith et al. [17] and can be interpreted as a beating between the oscillating molecular dipole and the electric field of the pulse tails [12]. The molecular dipole oscillates at a frequency very close to the atomic resonance since the excitation mainly occurs into highly excited vibrational levels which are strongly favored by high Franck-Condon factors.

For comparison the corresponding experimental transients for a non-symmetric and a more symmetric transmission band position are depicted in Figure 5. Even though the ion rate displays oscillations at positive delay, the signal fluctuations do not allow to significantly differentiate two distinct frequencies. But the measurement confirms clearly the earlier rise for the non-

symmetric band position leading to a maximum at 0 ps that decreases after the pump pulse. In accordance with the static measurements the maximum signal reached for both positions is in the same order of magnitude.

In summary, we observed coherent transient pump-probe signals for ultracold rubidium dimers with ultrashort shaped laser pulses. By reducing the bandwidth of the pump-pulse we performed spectrally resolved measurements of the transient signal at significant pump-probe delays. We compared the experimental results with quantum dynamical calculations and were able to explain the differing peak shapes for the investigated pump-probe delays in terms of the spectral positioning of the pulse.

This work was supported by the Deutsche Forschungsgemeinschaft in the framework of SFB 450, SPP 1116, and the Emmy Noether Programme (C. P. Koch).

## References

1. J. Weinstein, R. DeCarvalho, J. Kim, D. Patterson, B. Friedrich, J. Doyle, *Phys. Rev. A* **57**, 3173 (1998)
2. H. Bethlem, G. Berden, G. Meijer, *Phys. Rev. Lett.* **83**, 1558 (1999)
3. J. Herbig, T. Kraemer, M. Mark, T. Weber, C. Chin, H. Nagerl, R. Grimm, *Science* **301**, 1510 (2003)
4. H. Thorsheim, J. Weiner, P. Julienne, *Phys. Rev. Lett.* **58**, 2420 (1987)
5. A. Fioretti, D. Comparat, A. Crubellier, O. Dulieu, F. Masnou-Seeuws, P. Pillet, *Phys. Rev. Lett.* **80**, 4402 (1998)
6. K. Jones, E. Tiesinga, P. Lett, P. Julienne, *Rev. Mod. Phys.* **78**, 483 (2006)
7. M. Viteau, A. Chotia, M. Allegrini, N. Bouloufa, O. Dulieu, D. Comparat, P. Pillet, *Science* **321**, 232 (2008)
8. W. Salzmänn, U. Poschinger, R. Wester, M. Weidemüller, A. Merli, S. Weber, F. Sauer, M. Plewicky, F. Weise, A.M. Esparza, L. Wöste, A. Lindinger, *Phys. Rev. A* **73**, 023414 (2006)
9. B. Brown, A. Dicks, I. Walmsley, *Phys. Rev. Lett.* **96**, 173002 (2006)
10. F. Fatemi, K. Jones, H. Wang, I. Walmsley, P. Lett, *Phys. Rev. A* **64**, 033421 (2001)
11. G. Veshapidze, M.L. Trachy, H.U. Jang, C.W. Fehrenbach, B.D. DePaola, *Phys. Rev. A* **76**, R051401 (2007)
12. W. Salzmänn, T. Mullins, J. Eng, M. Albert, R. Wester, M. Weidemüller, A. Merli, S. Weber, F. Sauer, M. Plewicky, F. Weise, L. Wöste, A. Lindinger, *Phys. Rev. Lett.* **100**, 233003 (2008)
13. J. Petrovic, D. McCabe, D. England, H. Martay, M. Friedman, A. Dicks, E. Dimovab, I. Walmsley, *Faraday Discuss.* **142**, 1 (2009)
14. C. Townsend, N. Edwards, K. Zetie, C. Cooper, J. Rink, C. Foot, *Phys. Rev. A* **53**, 1702 (1996)
15. C. Koch, R. Kosloff, F. Masnou-Seeuws, *Phys. Rev. A* **73**, 043409 (2006)
16. N. Dudovich, D. Oron, Y. Silberberg, *Phys. Rev. Lett.* **88**, 123004 (2002)
17. S. Zamith, J. Degert, S. Stock, B. de Beauvoir, V. Blanchet, M.A. Bouchene, B. Girard, *Phys. Rev. Lett.* **87**, 033001 (2001)